

# Robust high-order low-rank BUG integrators based on explicit Runge-Kutta methods

Fabio Nobile<sup>1</sup> and Sébastien Riffaud<sup>1\*</sup>

<sup>1</sup>CSQI Chair, École Polytechnique Fédérale de Lausanne, 1015  
Lausanne, Switzerland.

\*Corresponding author(s). E-mail(s): [sebastien.riffaud@epfl.ch](mailto:sebastien.riffaud@epfl.ch);

## Abstract

In this work, we propose high-order basis-update & Galerkin (BUG) integrators based on explicit Runge-Kutta methods for large-scale matrix differential equations. These dynamical low-rank integrators are high-order extensions of the BUG integrator [1] and are constructed by performing one time-step of the first-order BUG integrator at each stage of the Runge-Kutta method. In this way, the resulting Runge-Kutta BUG integrator is robust to the presence of small singular values and does not involve backward time-integration steps. We provide an error bound, which shows that the Runge-Kutta BUG integrator retains the order of convergence of the associated Runge-Kutta method until the error reaches a plateau corresponding to the low-rank truncation and which vanishes as the rank increases. This error bound is finally validated numerically on three different test cases. The results demonstrate the high-order convergence of the Runge-Kutta BUG integrator and its superior accuracy compared to other low-rank integrators proposed in the literature.

**Keywords:** Dynamical low-rank approximation, Matrix differential equations

## 1 Introduction

Dynamical low-rank approximations (DLRAs) enable a significant reduction in the computational cost associated with numerical integration of large-scale matrix differential equations:

$$\dot{\mathbf{A}} = \mathbf{F}(t, \mathbf{A}), \quad \mathbf{A}(0) = \mathbf{A}_0 \in \mathbb{R}^{n \times m}, \quad (1)$$

which appear in many applications, such as kinetic equations [2–8] due to the large phase space, in stochastic simulations [9–17] which require to solve the differential equation for a large number of random realizations, or in sequential parameter estimation [18–21] due to the evaluation of the solution for different parameter values. The main idea of DLRAs consists in approximating the solution  $\mathbf{A}$  by a low-rank matrix  $\mathbf{Y}$  in an SVD-like form:

$$\mathbf{Y}(t) = \mathbf{U}(t)\mathbf{S}(t)\mathbf{V}(t)^T \in \mathbb{R}^{n \times m}, \quad (2)$$

where  $\mathbf{U} \in \mathbb{R}^{n \times r}$  and  $\mathbf{V} \in \mathbb{R}^{m \times r}$  are orthonormal matrices, and  $\mathbf{S} \in \mathbb{R}^{r \times r}$  is a square invertible matrix (not necessarily diagonal) with  $r \ll n, m$  denoting the rank.

A challenging issue concerns the time-integration of the different factors  $\mathbf{U}$ ,  $\mathbf{S}$ , and  $\mathbf{V}$ . Perhaps the most intuitive approach is to consider the differential equations derived in [22] and governing the evolution of the low-rank factorization over time:

$$\begin{cases} \dot{\mathbf{U}} = (\mathbf{I} - \mathbf{U}\mathbf{U}^T) \mathbf{F}(t, \mathbf{Y}) \mathbf{V} \mathbf{S}^{-1} \\ \dot{\mathbf{S}} = \mathbf{U}^T \mathbf{F}(t, \mathbf{Y}) \mathbf{V} \\ \dot{\mathbf{V}} = (\mathbf{I} - \mathbf{V}\mathbf{V}^T) \mathbf{F}(t, \mathbf{Y})^T \mathbf{U} \mathbf{S}^{-T}, \end{cases} \quad (3)$$

where we have assumed that  $\mathbf{U}^T \dot{\mathbf{U}} = \mathbf{V}^T \dot{\mathbf{V}} = \mathbf{0}$ . Unfortunately, this system involves the inverse of  $\mathbf{S}$ , which can cause severe time-step size restrictions if the singular values of  $\mathbf{S}$  are small, since the step size of standard time-integration schemes must be proportional to the smallest nonzero singular value. An alternative formulation to (3) is obtained by projecting the matrix differential equation (1) onto the tangent space of the manifold  $\mathcal{M}_r$  of rank- $r$  matrices:

$$\dot{\mathbf{Y}} = \mathbf{P}_r(\mathbf{Y}) \mathbf{F}(t, \mathbf{Y}), \quad \mathbf{Y}(0) = \mathbf{Y}_0 \in \mathcal{M}_r, \quad (4)$$

where

$$\mathbf{P}_r(\mathbf{Y}) \mathbf{Z} = \mathbf{U}\mathbf{U}^T \mathbf{Z} - \mathbf{U}\mathbf{U}^T \mathbf{Z} \mathbf{V} \mathbf{V}^T + \mathbf{Z} \mathbf{V} \mathbf{V}^T \quad (5)$$

stands for the orthogonal projection of  $\mathbf{Z} \in \mathbb{R}^{n \times m}$  onto the tangent space at  $\mathbf{Y} \in \mathcal{M}_r$ . In the projection-splitting integrator [23, 24], this tangent-space projection is split into three alternating subprojections using the Lie-Trotter or Strang splitting. The resulting low-rank integrator is robust to the presence of small singular values, but the step associated with the update of  $\mathbf{S}$  integrates the solution backward in time, which can lead to instabilities for parabolic and hyperbolic problems [25].

In recent years, several low-rank integrators that are robust to the presence of small singular values and do not involve backward time-integration steps have been proposed:

- the basis-update & Galerkin (BUG) integrators [1, 26, 27], where  $\mathbf{U}$  and  $\mathbf{V}$  are first updated using the tangent-space projection, and then  $\mathbf{S}$  is updated using a Galerkin projection of the matrix differential equation (1) onto the updated bases  $\mathbf{U}$  and  $\mathbf{V}$ ;

- the projected Runge-Kutta methods [28, 29], in which the projected differential equation (4) is integrated using a Runge-Kutta method which includes a truncation step that maintains low-rank approximations.

The convergence of the BUG integrator is limited to order one, but recent efforts are made to extend this low-rank integrator to higher orders. For instance, second-order extensions based on the midpoint rule have been proposed in [30, 31]. On the other hand, projected Runge-Kutta methods have second-order and high-order error bounds for time-explicit discretizations. However, these low-rank integrators do not share the favourable conservation properties offered by the Galerkin projection of the BUG integrator [32].

In this work, we propose high-order BUG integrators based on explicit Runge-Kutta methods. These low-rank integrators are high-order extensions of the BUG integrator and are constructed by performing one time-step of the first-order BUG integrator at each stage of the Runge-Kutta method. In this way, the resulting low-rank integrators are robust to the presence of small singular values and do not involve backward time-integration step. Moreover, compared with projected Runge-Kutta methods, the only difference is that the tangent-space projection is replaced by the Galerkin projection of the BUG integrator. Consequently, Runge-Kutta BUG integrators present two advantages. First, conservation properties can be preserved thanks to the Galerkin projection. Second, Runge-Kutta BUG integrators often provide better approximations than projected Runge-Kutta methods, since the Galerkin projection is more accurate than the tangent-space projection for approximating the solution at the discrete level. Then, we prove an error bound which shows that Runge-Kutta BUG integrators retain the order of convergence of the associated Runge-Kutta method until the error reaches a plateau corresponding to the rank truncation error and which vanishes as the rank increases. In particular, this property holds for any explicit Runge-Kutta method, allowing in practice the construction of various high-order low-rank integrators.

The remainder of the paper is organized as follows. Section 2 introduces the first-order BUG integrator based on the forward Euler method. In Section 3, we present high-order extensions of the BUG integrator based on explicit Runge-Kutta methods. Then, Section 4 analyzes the convergence of the proposed low-rank integrators. In Section 5, the resulting error bound is validated experimentally on three numerical test cases. Finally, Section 6 draws some conclusions and perspectives.

## 2 Recap: the BUG integrator based on the forward Euler method

The proposed low-rank integrator is an extension of the first-order BUG integrator [1]. For the convenience of the reader, we start by presenting the latter in the time-explicit case, i.e. for the forward Euler method. Let the time be discretized using a fixed time-step size  $h$ . The integration of the rank- $r$  solution  $\mathbf{Y}_k = \mathbf{U}_k \mathbf{S}_k \mathbf{V}_k^T$  from time  $t_k$  to  $t_k + h$  reads:

1. **K-step:** Assemble

$$\mathbf{K} = [\mathbf{U}_k, \mathbf{F}(t_k, \mathbf{Y}_k)\mathbf{V}_k] \in \mathbb{R}^{n \times 2r}, \quad (6)$$

and compute the augmented basis  $\widehat{\mathbf{U}}_{k+1}$  from the thin QR decomposition of  $\mathbf{K} = \widehat{\mathbf{U}}_{k+1}\mathbf{R}_K$ .

2. **L-step:** Assemble

$$\mathbf{L} = [\mathbf{V}_k, \mathbf{F}(t_k, \mathbf{Y}_k)^T\mathbf{U}_k] \in \mathbb{R}^{m \times 2r}, \quad (7)$$

and compute the augmented basis  $\widehat{\mathbf{V}}_{k+1}$  from the thin QR decomposition of  $\mathbf{L} = \widehat{\mathbf{V}}_{k+1}\mathbf{R}_L$ .

3. **S-step:** Set

$$\widehat{\mathbf{S}}_{k+1} = \widehat{\mathbf{U}}_{k+1}^T [\mathbf{Y}_k + h\mathbf{F}(t_k, \mathbf{Y}_k)] \widehat{\mathbf{V}}_{k+1} \in \mathbb{R}^{2r \times 2r}. \quad (8)$$

4. **Truncation step:** Let the  $r$ -truncated singular value decomposition (SVD) of  $\widehat{\mathbf{S}}_{k+1}$  be  $\widehat{\mathbf{\Phi}} \mathbf{\Sigma} \widehat{\mathbf{\Psi}}^T$ , where  $\widehat{\mathbf{\Phi}}, \widehat{\mathbf{\Psi}} \in \mathbb{R}^{2r \times r}$  are orthonormal matrices, and  $\mathbf{\Sigma} \in \mathbb{R}^{r \times r}$  is a diagonal matrix with non-negative real numbers on the diagonal. Set

$$\begin{aligned} \mathbf{U}_{k+1} &= \widehat{\mathbf{U}}_{k+1} \widehat{\mathbf{\Phi}}, \\ \mathbf{S}_{k+1} &= \mathbf{\Sigma}, \\ \mathbf{V}_{k+1} &= \widehat{\mathbf{V}}_{k+1} \widehat{\mathbf{\Psi}}. \end{aligned} \quad (9)$$

In order to simplify notation, let  $\llbracket \mathbf{X} \rrbracket_r$  denote the projection of  $\mathbf{X}$  onto  $\mathcal{M}_r$ , which is given by truncating the SVD of  $\mathbf{X}$ . Moreover, let  $\text{ortho}(\mathbf{X})$  denote an orthogonal matrix spanning the range of  $\mathbf{X}$ , which can be obtained from the pivoted QR decomposition of  $\mathbf{X}$ . The BUG integrator based on the forward Euler method is summarized in Algorithm 1. Note that the rank has been fixed here for simplicity, but an adaptive rank can also be used to truncate the augmented solution  $\widehat{\mathbf{Y}}_{k+1}$ .

### 3 Extension of the BUG integrator to high-order explicit Runge-Kutta methods

We now extend the BUG integrator to high-order explicit Runge-Kutta methods. Let's consider the explicit Runge-Kutta method:

$$\begin{aligned} \mathbf{Z}_{(i)} &= \mathbf{Z}_k + h \sum_{j=1}^{i-1} a_{i,j} \mathbf{F}(t_k + hc_j, \mathbf{Z}_{(j)}), \quad i = 1, \dots, s, \\ \mathbf{Z}_{k+1} &= \mathbf{Z}_k + h \sum_{i=1}^s b_i \mathbf{F}(t_k + hc_i, \mathbf{Z}_{(i)}), \end{aligned} \quad (10)$$

where examples of Butcher tableaux are provided in Appendix A. The main idea is to perform one time-step of the BUG integrator at each stage of the Runge-Kutta method. To this end, the key point concerns the definition of the augmented bases.

Consider, for example, the final stage with the initial value  $\mathbf{Z}_k = \mathbf{Y}_k$ :

$$\mathbf{Y}_{k+1} = \mathbf{Y}_k + h \sum_{i=1}^s b_i \mathbf{F}(t_k + hc_i, \mathbf{Y}_{(i)}).$$

The augmented bases  $\widehat{\mathbf{U}}_{k+1}$  and  $\widehat{\mathbf{V}}_{k+1}$  are constructed here to represent exactly  $\mathbf{Y}_k$  and the tangent-space projection of the different terms  $b_i \mathbf{F}(t_k + hc_i, \mathbf{Y}_{(i)})$  for  $i \in \{1, \dots, s\}$ . Notably,  $\mathbf{Y}_k$  is represented on the left and right bases  $\mathbf{U}_k$  and  $\mathbf{V}_k$ , while the tangent-space projection of  $\mathbf{F}(t_k + hc_i, \mathbf{Y}_{(i)})$  is represented on  $[\mathbf{U}_{(i)}, \mathbf{F}_{(i)} \mathbf{V}_{(i)}]$  and  $[\mathbf{V}_{(i)}, \mathbf{F}_{(i)}^T \mathbf{U}_{(i)}]$ , with  $\mathbf{F}_{(i)} = \mathbf{F}(t_k + hc_i, \mathbf{Y}_{(i)})$ , according to equation (5). Moreover, let's introduce the coefficients  $\alpha_{i,j}$  and  $\beta_i$ , defined as

$$\alpha_{i,j} = \begin{cases} 1 & \text{if } a_{i,j} \neq 0 \\ 0 & \text{otherwise} \end{cases} \quad \text{and} \quad \beta_i = \begin{cases} 1 & \text{if } b_i \neq 0 \\ 0 & \text{otherwise,} \end{cases}$$

which will allow us to discard the bases that are not involved in the different tangent-space projections. The augmented bases  $\widehat{\mathbf{U}}_{k+1}$  and  $\widehat{\mathbf{V}}_{k+1}$  are given by

$$\begin{aligned} \widehat{\mathbf{U}}_{k+1} &\leftarrow \text{ortho}([\mathbf{U}_k, \beta_1 \mathbf{U}_{(1)}, \beta_1 \mathbf{F}_{(1)} \mathbf{V}_{(1)}, \dots, \beta_s \mathbf{U}_{(s)}, \beta_s \mathbf{F}_{(s)} \mathbf{V}_{(s)}]), \\ \widehat{\mathbf{V}}_{k+1} &\leftarrow \text{ortho}([\mathbf{V}_k, \beta_1 \mathbf{V}_{(1)}, \beta_1 \mathbf{F}_{(1)}^T \mathbf{U}_{(1)}, \dots, \beta_s \mathbf{V}_{(s)}, \beta_s \mathbf{F}_{(s)}^T \mathbf{U}_{(s)}]), \end{aligned}$$

where the terms  $\beta_1 \mathbf{U}_{(1)}$  and  $\beta_1 \mathbf{V}_{(1)}$  can be removed since  $\mathbf{U}_{(1)} = \mathbf{U}_k$  and  $\mathbf{V}_{(1)} = \mathbf{V}_k$ . The Runge-Kutta BUG integrator corresponding to (10) is finally described in Algorithm 2. As mentioned previously, an adaptative rank can also be used to ensure that the truncation error is smaller than a prescribed tolerance.

**Remark 1.** *The rank of the augmented solution  $\widehat{\mathbf{Y}}_{k+1}$  (resp.  $\widehat{\mathbf{Y}}_{(i+1)}$ ) is at most  $2rs$  (resp.  $2ri$ ).*

**Remark 2.** *When  $r = \min\{n, m\}$ , the Runge-Kutta BUG integrator is equivalent to the associated Runge-Kutta method, since the manifold  $\mathcal{M}_r$  corresponds to the whole Euclidean space  $\mathbb{R}^{n \times m}$ , and there is therefore no projection or truncation error.*

---

**Algorithm 1** First-order BUG integrator [1] based on the forward Euler method

---

**Input:**  $\mathbf{Y}_0$ .

**Output:**  $\mathbf{Y}_1, \dots, \mathbf{Y}_{N_t}$ .

- 1: **for**  $k = 0, \dots, N_t - 1$  **do**
  - 2:    $\mathbf{Y}_k := \mathbf{U}_k \mathbf{S}_k \mathbf{V}_k^T$ ;
  - 3:    $\mathbf{F}_k \leftarrow \mathbf{F}(t_k, \mathbf{Y}_k)$ ;
  - 4:    $\widehat{\mathbf{U}}_{k+1} \leftarrow \text{ortho}([\mathbf{U}_k, \mathbf{F}_k \mathbf{V}_k])$ ; ▷ K-step (6)
  - 5:    $\widehat{\mathbf{V}}_{k+1} \leftarrow \text{ortho}([\mathbf{V}_k, \mathbf{F}_k^T \mathbf{U}_k])$ ; ▷ L-step (8)
  - 6:    $\widehat{\mathbf{S}}_{k+1} \leftarrow \widehat{\mathbf{U}}_{k+1}^T [\mathbf{Y}_k + h \mathbf{F}_k] \widehat{\mathbf{V}}_{k+1}$ ; ▷ S-step (7)
  - 7:    $\widehat{\mathbf{Y}}_{k+1} \leftarrow \widehat{\mathbf{U}}_{k+1} \widehat{\mathbf{S}}_{k+1} \widehat{\mathbf{V}}_{k+1}^T$ .
  - 8:    $\mathbf{Y}_{k+1} \leftarrow \llbracket \widehat{\mathbf{Y}}_{k+1} \rrbracket_r$ . ▷ Truncation step (9)
  - 9: **end**
-

---

**Algorithm 2** High-order explicit Runge-Kutta BUG integrator
 

---

**Input:**  $\mathbf{Y}_0$ .

**Output:**  $\mathbf{Y}_1, \dots, \mathbf{Y}_{N_t}$ .

```

1: for  $k = 0, \dots, N_t - 1$  do
2:    $\mathbf{Y}_{(1)} \leftarrow \mathbf{Y}_k$ ;
3:   for  $i = 1, \dots, s - 1$  do
4:      $\mathbf{Y}_{(i)} := \mathbf{U}_{(i)} \mathbf{S}_{(i)} \mathbf{V}_{(i)}^T$ ;
5:      $\mathbf{F}_{(i)} \leftarrow \mathbf{F}(t_k + hc_i, \mathbf{Y}_{(i)})$ ;
6:      $\widehat{\mathbf{U}}_{(i+1)} \leftarrow \text{ortho}([\mathbf{U}_k, \alpha_{i+1,1} \mathbf{F}_{(1)} \mathbf{V}_{(1)}, \dots, \alpha_{i+1,i} \mathbf{U}_{(i)}, \alpha_{i+1,i} \mathbf{F}_{(i)} \mathbf{V}_{(i)}]);$ 
7:      $\widehat{\mathbf{V}}_{(i+1)} \leftarrow \text{ortho}([\mathbf{V}_k, \alpha_{i+1,1} \mathbf{F}_{(1)}^T \mathbf{U}_{(1)}, \dots, \alpha_{i+1,i} \mathbf{V}_{(i)}, \alpha_{i+1,i} \mathbf{F}_{(i)}^T \mathbf{U}_{(i)}]);$ 
8:      $\widehat{\mathbf{S}}_{(i+1)} \leftarrow \widehat{\mathbf{U}}_{(i+1)}^T [\mathbf{Y}_k + h(a_{i+1,1} \mathbf{F}_{(1)} + \dots + a_{i+1,i} \mathbf{F}_{(i)})] \widehat{\mathbf{V}}_{(i+1)}$ ;
9:      $\widehat{\mathbf{Y}}_{(i+1)} \leftarrow \widehat{\mathbf{U}}_{(i+1)} \widehat{\mathbf{S}}_{(i+1)} \widehat{\mathbf{V}}_{(i+1)}^T$ ;
10:     $\mathbf{Y}_{(i+1)} \leftarrow \llbracket \widehat{\mathbf{Y}}_{(i+1)} \rrbracket_r$ ;
11:  end
12:   $\mathbf{Y}_{(s)} := \mathbf{U}_{(s)} \mathbf{S}_{(s)} \mathbf{V}_{(s)}^T$ ;
13:   $\mathbf{F}_{(s)} \leftarrow \mathbf{F}(t_k + hc_s, \mathbf{Y}_{(s)})$ ;
14:   $\widehat{\mathbf{U}}_{k+1} \leftarrow \text{ortho}([\mathbf{U}_k, \beta_1 \mathbf{F}_{(1)} \mathbf{V}_{(1)}, \dots, \beta_s \mathbf{U}_{(s)}, \beta_s \mathbf{F}_{(s)} \mathbf{V}_{(s)}]);$ 
15:   $\widehat{\mathbf{V}}_{k+1} \leftarrow \text{ortho}([\mathbf{V}_k, \beta_1 \mathbf{F}_{(1)}^T \mathbf{U}_{(1)}, \dots, \beta_s \mathbf{V}_{(s)}, \beta_s \mathbf{F}_{(s)}^T \mathbf{U}_{(s)}]);$ 
16:   $\widehat{\mathbf{S}}_{k+1} \leftarrow \widehat{\mathbf{U}}_{k+1}^T [\mathbf{Y}_k + h(b_1 \mathbf{F}_{(1)} + \dots + b_s \mathbf{F}_{(s)})] \widehat{\mathbf{V}}_{k+1}$ ;
17:   $\widehat{\mathbf{Y}}_{k+1} \leftarrow \widehat{\mathbf{U}}_{k+1} \widehat{\mathbf{S}}_{k+1} \widehat{\mathbf{V}}_{k+1}^T$ .
18:   $\mathbf{Y}_{k+1} \leftarrow \llbracket \widehat{\mathbf{Y}}_{k+1} \rrbracket_r$ .
19: end

```

---

## 4 Convergence analysis

In this section, we analyze the convergence of the Runge-Kutta BUG integrator for a fixed rank  $r$ . This analysis is based on two assumptions. The first assumption is used in the first-order BUG integrator [1] and implies, in particular, the existence and uniqueness of the solution to (1) according to the Picard-Lindelöf theorem, while the second assumption is required in Theorem 3.1 of [33] to analyze the local error of high-order Runge-Kutta methods. Furthermore, the present analysis is done in the Frobenius norm, and  $\|\cdot\|_F$  will stand for the Frobenius norm in the following.

**Assumption 1.**  $\mathbf{F}$  is Lipschitz continuous and bounded: there exists a Lipschitz constant  $L > 0$  and a constant  $B > 0$  such that

$$\|\mathbf{F}(t, \mathbf{X}) - \mathbf{F}(t, \mathbf{Z})\|_F \leq L \|\mathbf{X} - \mathbf{Z}\|_F \quad \text{and} \quad \|\mathbf{F}(t, \mathbf{X})\|_F \leq B$$

for all  $\mathbf{X}, \mathbf{Z} \in \mathbb{R}^{n \times m}$  and  $0 \leq t \leq T$ .

**Assumption 2.** Let  $\Phi_{\mathbf{F}}^t$  denote the exact flow of  $\mathbf{F}$  (i.e., the mapping such that  $\mathbf{A}(t) = \Phi_{\mathbf{F}}^t(\mathbf{A}_0)$ ). When considering a Runge-Kutta method of order  $p$ , the first  $p$

derivatives

$$\frac{d^q}{dt^q} \Phi_{\mathbf{F}}^t(\mathbf{X}), \quad q = 1, \dots, p,$$

exist (and are continuous) for all  $\mathbf{X} \in \mathbb{R}^{n \times m}$ .

#### 4.1 Error estimation

We start by introducing several definitions and lemmata that will be useful to prove the high-order convergence of the Runge-Kutta BUG integrator. In particular, Lemma 2 shows that the projection error resulting from the Galerkin projection of the Runge-Kutta BUG integrator is not larger than the one resulting from the tangent-space projection, which will allow us to adapt the convergence analysis of the projected Runge-Kutta methods [28] to our Runge-Kutta BUG integrator. In addition, Definition 2 provides an estimate for the truncation error which will allow us to obtain error bounds with an improved order of convergence compared to [28].

**Lemma 1.** *Suppose that Assumption 1 holds. The exact flow is  $e^{Lt}$ -Lipschitz continuous:*

$$\|\Phi_{\mathbf{F}}^t(\mathbf{X}) - \Phi_{\mathbf{F}}^t(\mathbf{Z})\|_F \leq e^{Lt} \|\mathbf{X} - \mathbf{Z}\|_F \quad (11)$$

for all  $\mathbf{X}, \mathbf{Z} \in \mathbb{R}^{n \times m}$  and  $0 \leq t \leq T$ .

*Proof.* From Assumption 1, we derive the differential inequality

$$\begin{aligned} \frac{1}{2} \frac{d}{dt} \|\Phi_{\mathbf{F}}^t(\mathbf{X}) - \Phi_{\mathbf{F}}^t(\mathbf{Z})\|_F^2 &= \langle \Phi_{\mathbf{F}}^t(\mathbf{X}) - \Phi_{\mathbf{F}}^t(\mathbf{Z}), \mathbf{F}(t, \Phi_{\mathbf{F}}^t(\mathbf{X})) - \mathbf{F}(t, \Phi_{\mathbf{F}}^t(\mathbf{Z})) \rangle_F \\ &\leq L \|\Phi_{\mathbf{F}}^t(\mathbf{X}) - \Phi_{\mathbf{F}}^t(\mathbf{Z})\|_F^2, \end{aligned}$$

which can be rewritten as follows:

$$\frac{d}{dt} \|\Phi_{\mathbf{F}}^t(\mathbf{X}) - \Phi_{\mathbf{F}}^t(\mathbf{Z})\|_F \leq L \|\Phi_{\mathbf{F}}^t(\mathbf{X}) - \Phi_{\mathbf{F}}^t(\mathbf{Z})\|_F.$$

Then, according to the Grönwall's inequality, the exact flow verifies

$$\|\Phi_{\mathbf{F}}^t(\mathbf{X}) - \Phi_{\mathbf{F}}^t(\mathbf{Z})\|_F \leq e^{Lt} \|\mathbf{X} - \mathbf{Z}\|_F,$$

which concludes the proof.  $\square$

**Lemma 2.** *The Galerkin projection of the Runge-Kutta BUG integrator is more accurate than the tangent-space projection for approximating  $\mathbf{F}_{(i)}$ :*

$$\left\| \mathbf{F}_{(i)} - \widehat{\mathbf{U}}_{k+1} \widehat{\mathbf{U}}_{k+1}^T \mathbf{F}_{(i)} \widehat{\mathbf{V}}_{k+1} \widehat{\mathbf{V}}_{k+1}^T \right\|_F \leq \left\| \mathbf{F}_{(i)} - \mathbf{P}_r(\mathbf{Y}_{(i)}) \mathbf{F}_{(i)} \right\|_F \quad (12)$$

for all  $i \in \{1, \dots, s\}$  such that  $b_i \neq 0$ . Similarly, the projection error at each stage  $i \in \{1, \dots, s-1\}$  verifies

$$\left\| \mathbf{F}_{(j)} - \widehat{\mathbf{U}}_{(i+1)} \widehat{\mathbf{U}}_{(i+1)}^T \mathbf{F}_{(j)} \widehat{\mathbf{V}}_{(i+1)} \widehat{\mathbf{V}}_{(i+1)}^T \right\|_F \leq \left\| \mathbf{F}_{(j)} - \mathbf{P}_r(\mathbf{Y}_{(j)}) \mathbf{F}_{(j)} \right\|_F \quad (13)$$

for all  $j \in \{1, \dots, i\}$  such that  $a_{i+1,j} \neq 0$ .

*Proof.* We prove equation (12). The proof of equation (13) follows from the same arguments and is therefore omitted. Let the SVD of  $\mathbf{P}_r(\mathbf{Y}_{(i)})\mathbf{F}_{(i)}$  be  $\Phi \Sigma \Psi^T$ , where  $\Phi \in \mathbb{R}^{n \times \bar{r}}$  and  $\Psi \in \mathbb{R}^{m \times \bar{r}}$  are orthonormal matrices,  $\Sigma \in \mathbb{R}^{\bar{r} \times \bar{r}}$  is a diagonal matrix with non-negative real numbers on the diagonal, and  $\bar{r} \in \{r, \dots, \min\{n, m, 2r\}\}$ . If  $b_i \neq 0$ , then the augmented bases  $\widehat{\mathbf{U}}_{k+1}$  and  $\widehat{\mathbf{V}}_{k+1}$  contain by construction the range of  $[\mathbf{U}_{(i)}, \mathbf{F}_{(i)} \mathbf{V}_{(i)}]$  and  $[\mathbf{V}_{(i)}, \mathbf{F}_{(i)}^T \mathbf{U}_{(i)}]$ , respectively, and it follows that the left and right singular vectors of  $\mathbf{P}_r(\mathbf{Y}_{(i)})\mathbf{F}_{(i)}$  are included in the span of the augmented bases:

$$\Phi \subseteq \text{span}(\widehat{\mathbf{U}}_{k+1}) \quad \text{and} \quad \Psi \subseteq \text{span}(\widehat{\mathbf{V}}_{k+1}),$$

where  $\widehat{\mathbf{U}}_{k+1} \in \mathbb{R}^{n \times \widehat{r}}$ ,  $\widehat{\mathbf{V}}_{k+1} \in \mathbb{R}^{m \times \widehat{r}}$ , and  $\widehat{r} \in \{\bar{r}, \dots, \min\{n, m, 2rs\}\}$ . Consequently, the Galerkin projection onto the augmented bases verifies

$$\begin{aligned} \|\mathbf{F}_{(i)} - \mathbf{P}_r(\mathbf{Y}_{(i)})\mathbf{F}_{(i)}\|_F &= \|\mathbf{F}_{(i)} - \Phi \Sigma \Psi^T\|_F \\ &\geq \min_{\Sigma \in \mathbb{R}^{\bar{r} \times \bar{r}}} \|\mathbf{F}_{(i)} - \Phi \Sigma \Psi^T\|_F \\ &\geq \min_{\widehat{\Sigma} \in \mathbb{R}^{\widehat{r} \times \widehat{r}}} \|\mathbf{F}_{(i)} - \widehat{\mathbf{U}}_{k+1} \widehat{\Sigma} \widehat{\mathbf{V}}_{k+1}^T\|_F \\ &= \|\mathbf{F}_{(i)} - \widehat{\mathbf{U}}_{k+1} \widehat{\mathbf{U}}_{k+1}^T \mathbf{F}_{(i)} \widehat{\mathbf{V}}_{k+1} \widehat{\mathbf{V}}_{k+1}^T\|_F, \end{aligned}$$

which concludes the proof.  $\square$

**Definition 1.** As  $\mathbf{F}$  is bounded according to Assumption 1, the normal component of  $\mathbf{F}$  is also bounded and, consequently, there exists  $\varepsilon_r \geq 0$  such that the tangent-space projection error is bounded. Let

$$\varepsilon_r := \sup_{t \in [0, T]} \sup_{\mathbf{Y} \in \mathcal{M}_r} \|\mathbf{F}(t, \mathbf{Y}) - \mathbf{P}(\mathbf{Y})\mathbf{F}(t, \mathbf{Y})\|_F. \quad (14)$$

It follows that the error of the Galerkin projection onto the augmented bases is also bounded by  $\varepsilon_r$  according to Lemma 2. In addition, note that  $\varepsilon_r$  vanishes when  $r \rightarrow \min\{n, m\}$ .

**Lemma 3.** Suppose that Assumption 2 holds. The local error of a Runge-Kutta method of order  $p$  is bounded by

$$\left\| \mathbf{Z}_{k+1} - \Phi_{\mathbf{F}}^h(\mathbf{Z}_k) \right\|_F \leq C_L h^{p+1}, \quad \forall h \leq h_0, \quad (15)$$

where the constant  $C_L > 0$  is independent of  $h$ .

*Proof.* see Theorem 3.1 in Chapter 2 of [33].  $\square$



**Lemma 4.** *Suppose that Assumption 1 holds. The error resulting from the truncation step in the Runge-Kutta BUG integrator is proportional to  $h$ :*

$$\frac{1}{h} \left\| \widehat{\mathbf{Y}}_{k+1} - \left[ \widehat{\mathbf{Y}}_{k+1} \right]_r \right\|_F < \infty. \quad (16)$$

Similarly, the truncation error at each stage  $i \in \{1, \dots, s-1\}$  is proportional to  $h$ :

$$\frac{1}{h} \left\| \widehat{\mathbf{Y}}_{(i+1)} - \left[ \widehat{\mathbf{Y}}_{(i+1)} \right]_r \right\|_F < \infty. \quad (17)$$

*Proof.* We prove equation (16). The proof of equation (17) follows from the same arguments and is therefore omitted. Let  $\sigma_j(\mathbf{X})$  denote the  $j$ -th largest singular value of the matrix  $\mathbf{X} \in \mathbb{R}^{n \times m}$ . According to the Eckart-Young theorem [34], the squared truncation error is given by

$$\left\| \widehat{\mathbf{Y}}_{k+1} - \left[ \widehat{\mathbf{Y}}_{k+1} \right]_r \right\|_F^2 = \sum_{j=r+1}^{\min\{n, m, 2rs\}} \sigma_j^2(\widehat{\mathbf{Y}}_{k+1}), \quad (18)$$

since the rank of  $\widehat{\mathbf{Y}}_{k+1}$  is at most  $2rs$  (see Remark 1), and therefore  $\sigma_j^2(\widehat{\mathbf{Y}}_{k+1}) = 0$  for  $j \geq 2rs + 1$ . Then, according to Theorem 3.3.16 in [35], as

$$\widehat{\mathbf{Y}}_{k+1} = \mathbf{Y}_k + h \left( b_1 \widetilde{\mathbf{F}}_{(1)} + \dots + b_s \widetilde{\mathbf{F}}_{(s)} \right) \quad \text{with} \quad \widetilde{\mathbf{F}}_{(i)} = \widehat{\mathbf{U}}_{k+1} \widehat{\mathbf{U}}_{k+1}^T \mathbf{F}_{(i)} \widehat{\mathbf{V}}_{k+1} \widehat{\mathbf{V}}_{k+1}^T,$$

the singular values of  $\widehat{\mathbf{Y}}_{k+1}$  are bounded by

$$\sigma_{i+j-1}(\widehat{\mathbf{Y}}_{k+1}) \leq \sigma_i(\mathbf{Y}_k) + h \sigma_j(b_1 \widetilde{\mathbf{F}}_{(1)} + \dots + b_s \widetilde{\mathbf{F}}_{(s)})$$

for all  $i \in \{1, \dots, \min\{n, m, 2r\}\}$  and  $j \in \{1, \dots, \min\{n, m, 2rs\}\}$  such that  $i+j-1 \leq \min\{n, m, 2rs\}$ . In particular, for  $i = r+1$  and  $j \geq 1$ , it follows that

$$\sigma_{r+j}(\widehat{\mathbf{Y}}_{k+1}) \leq h \sigma_j(b_1 \widetilde{\mathbf{F}}_{(1)} + \dots + b_s \widetilde{\mathbf{F}}_{(s)}), \quad (19)$$

since the rank of  $\mathbf{Y}_k$  is at most  $r$ . Moreover, from Assumption 1, we deduce that

$$\begin{aligned} \sum_{j=1}^{\min\{n, m, 2rs\}} \sigma_j^2(b_1 \widetilde{\mathbf{F}}_{(1)} + \dots + b_s \widetilde{\mathbf{F}}_{(s)}) &= \left\| b_1 \widetilde{\mathbf{F}}_{(1)} + \dots + b_s \widetilde{\mathbf{F}}_{(s)} \right\|_F^2 \\ &\leq \left( |b_1| \left\| \widetilde{\mathbf{F}}_{(1)} \right\|_F + \dots + |b_s| \left\| \widetilde{\mathbf{F}}_{(s)} \right\|_F \right)^2 \\ &\leq \left( |b_1| \left\| \mathbf{F}_{(1)} \right\|_F + \dots + |b_s| \left\| \mathbf{F}_{(s)} \right\|_F \right)^2 \\ &\leq \left( |b_1| B + \dots + |b_s| B \right)^2 \\ &= C_B^2 B^2, \end{aligned}$$

where  $C_B = \sum_{i=1}^s |b_i|$ . In particular, it follows that

$$\sigma_j^2(b_1\tilde{\mathbf{F}}_{(1)} + \dots + b_s\tilde{\mathbf{F}}_{(s)}) \leq C_B^2 B^2 \quad (20)$$

for all  $j \in \{1, \dots, \min\{n, m, 2rs\}\}$ . Finally, combining equations (18), (19), and (20) yields

$$\begin{aligned} \left\| \widehat{\mathbf{Y}}_{k+1} - \llbracket \widehat{\mathbf{Y}}_{k+1} \rrbracket_r \right\|_F^2 &= \sum_{j=1}^{\min\{n, m, 2rs\} - r} \sigma_{r+j}^2(\widehat{\mathbf{Y}}_{k+1}) \\ &\leq \sum_{j=1}^{\min\{n, m, 2rs\} - r} h^2 \sigma_j^2(b_1\tilde{\mathbf{F}}_{(1)} + \dots + b_s\tilde{\mathbf{F}}_{(s)}) \\ &\leq \sum_{j=1}^{\min\{n, m, 2rs\} - r} h^2 C_B^2 B^2 \\ &= h^2 (\min\{n, m, 2rs\} - r) C_B^2 B^2. \end{aligned}$$

The desired result follows directly from the fact that the term  $(\min\{n, m, 2rs\} - r)C_B^2 B^2$  is finite.  $\square$

**Definition 2.** According to Lemma 4, there exists  $\gamma_r \geq 0$  such that the ratios (16) and (17) are bounded. Let

$$\gamma_r := \max_{0 \leq k \leq N_t - 1} \sup_{\mathbf{Y} \in \mathcal{M}_r} \max_{1 \leq i \leq s} \frac{1}{h} \left\| \widehat{\mathbf{Y}}_{k,(i)} - \llbracket \widehat{\mathbf{Y}}_{k,(i)} \rrbracket_r \right\|_F, \quad (21)$$

where  $\widehat{\mathbf{Y}}_{k,(i)}$  denotes the solution  $\widehat{\mathbf{Y}}_{(i+1)}$  at time  $t_k$  with initial value  $\mathbf{Y}_k = \mathbf{Y}$  and with the definition  $\widehat{\mathbf{Y}}_{k,(s+1)} = \widehat{\mathbf{Y}}_{k+1}$ . It follows that the truncation error in the Runge-Kutta BUG integrator is bounded by

$$\left\| \widehat{\mathbf{Y}}_{k,(i)} - \llbracket \widehat{\mathbf{Y}}_{k,(i)} \rrbracket_r \right\|_F \leq h\gamma_r$$

for all  $k \in \{0, \dots, N_t - 1\}$ ,  $\mathbf{Y}_k = \mathbf{Y} \in \mathcal{M}_r$ , and  $i \in \{1, \dots, s\}$ . In addition, note that  $\gamma_r$  vanishes when  $r \rightarrow \min\{n, m\}$ .

**Lemma 5.** Consider the Runge-Kutta method (10) with the initial value  $\mathbf{Z}_k = \mathbf{Y}_k$ . Moreover, suppose that Assumption 1 holds. The local approximation error is bounded at each stage  $i \in \{1, \dots, s\}$  by

$$\left\| \mathbf{Y}_{(i)} - \mathbf{Z}_{(i)} \right\|_F \leq C_i h (\varepsilon_r + \gamma_r), \quad (22)$$

where the constant  $C_i > 0$  is independent of  $r$  and  $h$ .

*Proof.* We proceed by induction. For  $i = 1$ , the statement is trivial since  $\mathbf{Z}_{(1)} = \mathbf{Z}_k = \mathbf{Y}_k = \mathbf{Y}_{(1)}$ . Then, for  $i \in \{2, \dots, s\}$ , the local error can be split into

$$\|\mathbf{Y}_{(i)} - \mathbf{Z}_{(i)}\|_F \leq \|\mathbf{Y}_{(i)} - \widehat{\mathbf{Y}}_{(i)}\|_F + \|\widehat{\mathbf{Y}}_{(i)} - \mathbf{Z}_{(i)}\|_F. \quad (23)$$

The first term in the RHS is bounded according to Definition 2 by

$$\|\widehat{\mathbf{Y}}_{(i)} - \mathbf{Y}_{(i)}\|_F \leq h\gamma_r. \quad (24)$$

Regarding the second term, we deduce from Lemma 2, Definition 1, and the induction hypothesis that

$$\begin{aligned} \|\widehat{\mathbf{Y}}_{(i)} - \mathbf{Z}_{(i)}\|_F &\leq h \sum_{j=1}^{i-1} |a_{i,j}| \left\| \widehat{\mathbf{U}}_{(i)} \widehat{\mathbf{U}}_{(i)}^T \mathbf{F}(t_k + hc_j, \mathbf{Y}_{(j)}) \widehat{\mathbf{V}}_{(i)} \widehat{\mathbf{V}}_{(i)}^T - \mathbf{F}(t_k + hc_j, \mathbf{Z}_{(j)}) \right\|_F \\ &= h \sum_{\substack{j=1 \\ a_{i,j} \neq 0}}^{i-1} |a_{i,j}| \left\| \widehat{\mathbf{U}}_{(i)} \widehat{\mathbf{U}}_{(i)}^T \mathbf{F}(t_k + hc_j, \mathbf{Y}_{(j)}) \widehat{\mathbf{V}}_{(i)} \widehat{\mathbf{V}}_{(i)}^T - \mathbf{F}(t_k + hc_j, \mathbf{Z}_{(j)}) \right\|_F \\ &\leq h \sum_{\substack{j=1 \\ a_{i,j} \neq 0}}^{i-1} |a_{i,j}| \left( \left\| \widehat{\mathbf{U}}_{(i)} \widehat{\mathbf{U}}_{(i)}^T \mathbf{F}(t_k + hc_j, \mathbf{Y}_{(j)}) \widehat{\mathbf{V}}_{(i)} \widehat{\mathbf{V}}_{(i)}^T - \mathbf{F}(t_k + hc_j, \mathbf{Y}_{(j)}) \right\|_F \right. \\ &\quad \left. + \left\| \mathbf{F}(t_k + hc_j, \mathbf{Y}_{(j)}) - \mathbf{F}(t_k + hc_j, \mathbf{Z}_{(j)}) \right\|_F \right) \\ &\leq h \sum_{\substack{j=1 \\ a_{i,j} \neq 0}}^{i-1} |a_{i,j}| \left( \left\| \mathbf{P}_r(\mathbf{Y}_{(j)}) \mathbf{F}(t_k + hc_j, \mathbf{Y}_{(j)}) - \mathbf{F}(t_k + hc_j, \mathbf{Y}_{(j)}) \right\|_F \right. \\ &\quad \left. + \left\| \mathbf{F}(t_k + hc_j, \mathbf{Y}_{(j)}) - \mathbf{F}(t_k + hc_j, \mathbf{Z}_{(j)}) \right\|_F \right) \\ &\leq h \sum_{\substack{j=1 \\ a_{i,j} \neq 0}}^{i-1} |a_{i,j}| (\varepsilon_r + L \|\mathbf{Y}_{(j)} - \mathbf{Z}_{(j)}\|_F) \\ &\leq C_A h \varepsilon_r + h \sum_{\substack{j=1 \\ a_{i,j} \neq 0}}^{i-1} |a_{i,j}| LC_j h (\varepsilon_r + \gamma_r) \\ &\leq C_A h \varepsilon_r + h^2 (\varepsilon_r + \gamma_r) \sum_{\substack{j=1 \\ a_{i,j} \neq 0}}^{i-1} |a_{i,j}| LC_j \\ &\leq Ch \varepsilon_r + h^2 \gamma_r \sum_{\substack{j=1 \\ a_{i,j} \neq 0}}^{i-1} |a_{i,j}| LC_j, \end{aligned} \quad (25)$$

where  $C_A = \sum_{i,j=1}^s |a_{i,j}|$ , and the term  $\sum_{j=1, a_{i,j} \neq 0}^{i-1} |a_{i,j}| LC_j$ , associated with  $h^2$  and  $\varepsilon_r$ , has been absorbed in the constant  $C > 0$ . Finally, combining equations (23), (24), and (25) yields the desired result:

$$\begin{aligned} \|\mathbf{Y}_{(i)} - \mathbf{Z}_{(i)}\|_F &\leq Ch\varepsilon_r + h\gamma_r + h^2\gamma_r \sum_{\substack{j=1 \\ a_{i,j} \neq 0}}^{i-1} |a_{i,j}| LC_j \\ &\leq Ch\varepsilon_r + C'h\gamma_r \\ &\leq \max\{C, C'\}h(\varepsilon_r + \gamma_r), \end{aligned}$$

where the term  $\sum_{j=1, a_{i,j} \neq 0}^{i-1} |a_{i,j}| LC_j$ , associated with  $h^2$  and  $\gamma_r$ , has been absorbed in the constant  $C' > 0$ .  $\square$

## 4.2 Local and global error bounds

We now establish the local and global error bounds in Theorems 1 and 2, respectively. Compared with the bounds obtained in [28], the proposed Runge-Kutta BUG integrator retains the order of convergence of the associated Runge-Kutta method until the error reaches a plateau corresponding to the low-rank truncation and which vanishes as the rank increases. This is because we employ an additional estimate  $\gamma_r$  to bound the truncation error. In particular, by using this estimate and adapting the convergence analysis of [28], similar local and global error bounds can be proved for projected Runge-Kutta methods.

**Theorem 1.** *Suppose that Assumptions 1 and 2 hold. The local error of the Runge-Kutta BUG integrator is bounded by*

$$\left\| \mathbf{Y}_{k+1} - \Phi_{\mathbf{F}}^h(\mathbf{Y}_k) \right\|_F \leq C_{\text{loc}} h (\varepsilon_r + \gamma_r + h^p), \quad 0 \leq t_k = kh \leq T, \quad (26)$$

for all  $h \leq h_0$ . In particular, the constant  $C_{\text{loc}} > 0$  is independent of  $r$  and  $h$ .

*Proof.* We proceed in the same way as in Lemma 5. The local error can be split into

$$\begin{aligned} &\left\| \mathbf{Y}_{k+1} - \Phi_{\mathbf{F}}^h(\mathbf{Y}_k) \right\|_F \\ &\leq \left\| \mathbf{Y}_{k+1} - \widehat{\mathbf{Y}}_{k+1} \right\|_F + \left\| \widehat{\mathbf{Y}}_{k+1} - \mathbf{Z}_{k+1} \right\|_F + \left\| \mathbf{Z}_{k+1} - \Phi_{\mathbf{F}}^h(\mathbf{Y}_k) \right\|_F. \end{aligned} \quad (27)$$

The first term in the RHS is bounded according to Definition 2 by

$$\left\| \widehat{\mathbf{Y}}_{k+1} - \mathbf{Y}_{k+1} \right\|_F \leq h\gamma_r. \quad (28)$$

Regarding the second term, we deduce from Lemma 2, Definition 1, and Lemma 5 that

$$\begin{aligned}
\left\| \widehat{\mathbf{Y}}_{k+1} - \mathbf{Z}_{k+1} \right\|_F &\leq h \sum_{i=1}^s |b_i| \left\| \widehat{\mathbf{U}}_{k+1} \widehat{\mathbf{U}}_{k+1}^T \mathbf{F}(t_k + hc_i, \mathbf{Y}_{(i)}) \widehat{\mathbf{V}}_{k+1} \widehat{\mathbf{V}}_{k+1}^T - \mathbf{F}(t_k + hc_i, \mathbf{Z}_{(i)}) \right\|_F \\
&= h \sum_{\substack{i=1 \\ b_i \neq 0}}^s |b_i| \left\| \widehat{\mathbf{U}}_{k+1} \widehat{\mathbf{U}}_{k+1}^T \mathbf{F}(t_k + hc_i, \mathbf{Y}_{(i)}) \widehat{\mathbf{V}}_{k+1} \widehat{\mathbf{V}}_{k+1}^T - \mathbf{F}(t_k + hc_i, \mathbf{Z}_{(i)}) \right\|_F \\
&\leq h \sum_{\substack{i=1 \\ b_i \neq 0}}^s |b_i| \left( \left\| \widehat{\mathbf{U}}_{k+1} \widehat{\mathbf{U}}_{k+1}^T \mathbf{F}(t_k + hc_i, \mathbf{Y}_{(i)}) \widehat{\mathbf{V}}_{k+1} \widehat{\mathbf{V}}_{k+1}^T - \mathbf{F}(t_k + hc_i, \mathbf{Y}_{(i)}) \right\|_F \right. \\
&\quad \left. + \left\| \mathbf{F}(t_k + hc_i, \mathbf{Y}_{(i)}) - \mathbf{F}(t_k + hc_i, \mathbf{Z}_{(i)}) \right\|_F \right) \\
&\leq h \sum_{\substack{i=1 \\ b_i \neq 0}}^s |b_i| \left( \left\| \mathbf{P}_r(\mathbf{Y}_{(i)}) \mathbf{F}(t_k + hc_i, \mathbf{Y}_{(i)}) - \mathbf{F}(t_k + hc_i, \mathbf{Y}_{(i)}) \right\|_F \right. \\
&\quad \left. + \left\| \mathbf{F}(t_k + hc_i, \mathbf{Y}_{(i)}) - \mathbf{F}(t_k + hc_i, \mathbf{Z}_{(i)}) \right\|_F \right) \\
&\leq h \sum_{\substack{i=1 \\ b_i \neq 0}}^s |b_i| (\varepsilon_r + L \|\mathbf{Y}_{(i)} - \mathbf{Z}_{(i)}\|_F) \\
&\leq C_B h \varepsilon_r + h \sum_{\substack{i=1 \\ b_i \neq 0}}^s |b_i| LC_i h (\varepsilon_r + \gamma_r) \\
&\leq C_B h \varepsilon_r + h^2 (\varepsilon_r + \gamma_r) \sum_{\substack{i=1 \\ b_i \neq 0}}^s |b_i| LC_i \\
&\leq Ch \varepsilon_r + h^2 \gamma_r \sum_{\substack{i=1 \\ b_i \neq 0}}^s |b_i| LC_i,
\end{aligned} \tag{29}$$

where  $C_B = \sum_{i=1}^s |b_i|$ , and the term  $\sum_{i=1, b_i \neq 0}^s |b_i| LC_i$ , associated with  $h^2$  and  $\varepsilon_r$ , has been absorbed in the constant  $C > 0$ . The last term is bounded according to Lemma 3 by

$$\left\| \mathbf{Z}_{k+1} - \Phi_{\mathbf{F}}^h(\mathbf{Z}_k) \right\|_F \leq C_L h^{p+1}. \tag{30}$$

Finally, combining equations (27), (28), (29), and (30) yields the desired result:

$$\begin{aligned}
\left\| \mathbf{Y}_{k+1} - \Phi_{\mathbf{F}}^h(\mathbf{Y}_k) \right\|_F &\leq Ch \varepsilon_r + h \gamma_r + h^2 \gamma_r \sum_{\substack{i=1 \\ b_i \neq 0}}^s |b_i| LC_i + C_L h^{p+1} \\
&\leq Ch \varepsilon_r + C' h \gamma_r + C_L h^{p+1} \\
&\leq \max\{C, C', C_L\} h (\varepsilon_r + \gamma_r + h^p),
\end{aligned}$$

where the term  $\sum_{i=1, b_i \neq 0}^s |b_i| LC_i$ , associated with  $h^2$  and  $\gamma_r$ , has been absorbed in the constant  $C' > 0$ .  $\square$

**Theorem 2.** *Let the initial error be  $\delta_r = \|\mathbf{Y}_0 - \mathbf{A}_0\|_F$ , where the constant  $\delta_r$  vanishes when  $r \rightarrow \min\{n, m\}$ . Moreover, suppose that Assumptions 1 and 2 hold. The global error of the Runge-Kutta BUG integrator is bounded by*

$$\|\mathbf{Y}_k - \mathbf{A}(t_k)\|_F \leq C_{\text{glob}} (\delta_r + \varepsilon_r + \gamma_r + h^p), \quad 0 \leq t_k = kh \leq T, \quad (31)$$

for all  $h \leq h_0$ . In particular, the constant  $C_{\text{glob}} > 0$  is independent of  $r$  and  $h$ .

*Proof.* The bound results from the local error of Theorem 1 and the standard argument of Lady Windermere's fan with error propagation along the exact flow. More precisely, the global error can be expanded as the telescoping sum

$$\mathbf{Y}_k - \Phi_{\mathbf{F}}^{kh}(\mathbf{A}_0) = \left( \sum_{i=1}^k \Phi_{\mathbf{F}}^{(k-i)h}(\mathbf{Y}_k) - \Phi_{\mathbf{F}}^{(k-i+1)h}(\mathbf{Y}_{k-1}) \right) + \Phi_{\mathbf{F}}^{kh}(\mathbf{Y}_0) - \Phi_{\mathbf{F}}^{kh}(\mathbf{A}_0).$$

Then, the different terms can be bounded according to Lemma 1 and Theorem 1 by

$$\begin{aligned} \left\| \Phi_{\mathbf{F}}^{kh}(\mathbf{Y}_0) - \Phi_{\mathbf{F}}^{kh}(\mathbf{A}_0) \right\|_F &\leq e^{Lkh} \|\mathbf{Y}_0 - \mathbf{A}_0\|_F = e^{Lkh} \delta_r, \\ \left\| \Phi_{\mathbf{F}}^{(k-i)h}(\mathbf{Y}_k) - \Phi_{\mathbf{F}}^{(k-i)h}(\Phi_{\mathbf{F}}^h(\mathbf{Y}_{k-1})) \right\|_F &\leq e^{L(k-i)h} \left\| \mathbf{Y}_k - \Phi_{\mathbf{F}}^h(\mathbf{Y}_{k-1}) \right\|_F \\ &\leq e^{L(k-i)h} C_{\text{loc}} h (\varepsilon_r + \gamma_r + h^p), \end{aligned}$$

which leads to the upper bound:

$$\left\| \mathbf{Y}_k - \Phi_{\mathbf{F}}^{kh}(\mathbf{A}_0) \right\|_F \leq e^{Lkh} \delta_r + C_{\text{loc}} (\varepsilon_r + \gamma_r + h^p) \sum_{i=1}^k e^{L(k-i)h} h.$$

Finally, bounding the Riemann sum as

$$\sum_{i=1}^k h e^{L(k-i)h} \leq \int_0^{kh} e^{L(kh-t)} dt = \frac{e^{Lkh} - 1}{L}$$

and using  $kh \leq T$  yield the desired result:

$$\begin{aligned} \left\| \mathbf{Y}_k - \Phi_{\mathbf{F}}^{kh}(\mathbf{A}_0) \right\|_F &\leq e^{LT} \delta_r + C_{\text{loc}} \frac{e^{LT} - 1}{L} (\varepsilon_r + \gamma_r + h^p) \\ &\leq \max \left\{ e^{LT}, C_{\text{loc}} \frac{e^{LT} - 1}{L} \right\} (\delta_r + \varepsilon_r + \gamma_r + h^p). \end{aligned}$$

$\square$

**Remark 3.** If  $\delta_r, \varepsilon_r, \gamma_r \ll h^p$ , then the Runge-Kutta BUG integrator has the same order of convergence than the associated Runge-Kutta method. Otherwise, the error is proportional to the initial, projection, and truncation errors, which vanish as the rank increases.

## 5 Numerical experiments

According to Theorem 2, the rate of convergence of the proposed Runge-Kutta BUG integrator scales with  $h^p$  until the error reaches a plateau which vanishes as the rank increases. This theoretical result is verified numerically for three different experiments taken from [28, 36]. To this end, we investigate the convergence of several Runge-Kutta BUG integrators based on the following high-order explicit Runge-Kutta methods:

- midpoint method (RK2m);
- Heun’s method (RK2h);
- Heun’s third-order method (RK3h);
- third-order SSP RK method (RK3s);
- classic fourth-order Runge-Kutta method (RK4).

The accuracy of the resulting integrators is measured with respect to a reference solution  $\mathbf{A}_k$  computed using the fifth-order Runge-Kutta-Fehlberg method:

$$\text{Error} = \max_{0 \leq k \leq N_t} \|\mathbf{Y}_k - \mathbf{A}_k\|_F.$$

Furthermore, we compare these Runge-Kutta BUG integrators with the following state-of-the-art low-rank integrators:

- the first variant of the second-order BUG integrator (Midpoint BUG) of [30];
- the second-order projected Runge-Kutta method (PRK2h) [28];
- the third-order projected Runge-Kutta method (PRK3h) [28].

### 5.1 Allen-Cahn equation

We first consider the Allen-Cahn equation:

$$\begin{cases} \dot{\mathbf{A}}(t) = \theta(\mathbf{L}\mathbf{A}(t) + \mathbf{A}(t)\mathbf{L}) + \mathbf{A}(t) - \mathbf{A}(t) \odot \mathbf{A}(t) \odot \mathbf{A}(t) \\ \mathbf{A}(0) = \mathbf{A}_0, \end{cases}$$

where  $\mathbf{A}(t) \in \mathbb{R}^{n \times n}$ ,  $\mathbf{L} = \frac{n^2}{4\pi^2} \text{diag}(1, -2, 1) \in \mathbb{R}^{n \times n}$ ,  $t \in [0, 10]$ ,  $\theta = 10^{-2}$ , and  $\odot$  stands for the Hadamard product. The domain  $[0, 2\pi]^2$  is discretized using  $n = 128$  equidistant points in each direction, and the initial solution is given by

$$(\mathbf{A}_0)_{i,j} = \frac{\left[ e^{-\tan^2(x_i)} + e^{-\tan^2(y_j)} \right] \sin(x_i) \sin(y_j)}{1 + e^{|\csc(-x_i/2)|} + e^{|\csc(-y_j/2)|}}.$$

In Figure 1, we present the error of the Runge-Kutta BUG integrator as a function of the time-step size  $h$  and rank  $r$ . The reader can see that the Runge-Kutta BUG integrator achieves second-, third-, and fourth-order convergences until the error reaches a plateau corresponding to the low-rank truncation. This plateau decreases as the rank increases up to a certain limit, around  $10^{-9}$ , which is due to machine precision and results from the accumulation of rounding errors. In addition, the error of the Runge-Kutta BUG integrator is almost identical to that of the midpoint BUG integrator and projected Runge-Kutta methods.

## 5.2 Lyapunov equation

Then, we consider the Lyapunov equation:

$$\begin{cases} \dot{\mathbf{A}}(t) = \mathbf{L}\mathbf{A}(t) + \mathbf{A}(t)\mathbf{L} + \theta \frac{\mathbf{C}}{\|\mathbf{C}\|_F} \\ \mathbf{A}(0) = \mathbf{A}_0, \end{cases}$$

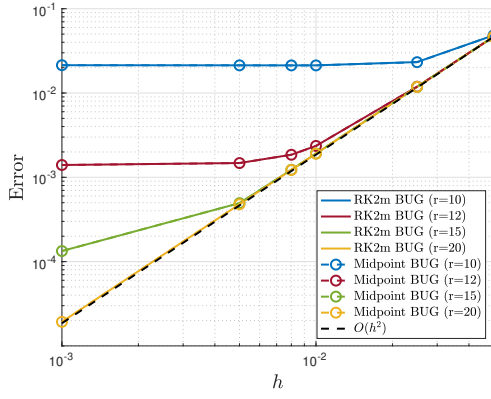
where  $\mathbf{A}(t) \in \mathbb{R}^{n \times n}$ ,  $\mathbf{L} = \frac{n^2}{4\pi^2} \text{diag}(1, -2, 1) \in \mathbb{R}^{n \times n}$ ,  $\mathbf{C} \in \mathbb{R}^{n \times n}$ ,  $t \in [0, 1]$ , and  $\theta \geq 0$ . The domain  $[-\pi, \pi]^2$  is discretized using  $n = 128$  equidistant points in each direction, and the initial solution and forcing term are given by

$$(\mathbf{A}_0)_{i,j} = \sin(x_i) \sin(y_j) \quad \text{and} \quad (\mathbf{C})_{i,j} = \sum_{l=1}^{11} 10^{-(l-1)} e^{-l(x_i^2 + y_j^2)}.$$

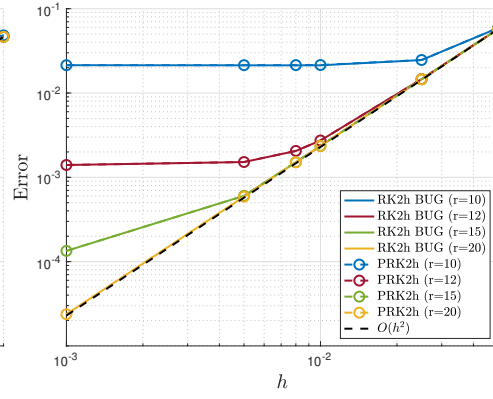
We start with the case  $\theta = 10^{-5}$ . In Figure 2, we fix the rank to  $r = 5$  and we report the error of the Runge-Kutta BUG integrator as a function of the time-step size  $h$ . The reader can see that the proposed integrator achieves second- and third-order convergences until the error reaches a limit, around  $10^{-10}$ , due to the machine precision. Regarding the fourth-order convergence, this one is not visible since the error is already of the order of  $10^{-11}$  for  $h = 5 \times 10^{-4}$ . Moreover, the error of the Runge-Kutta BUG integrator is almost the same as that of the midpoint BUG integrator and projected Runge-Kutta methods.

We now consider the case  $\theta = 1$ , where a higher rank is necessary to obtain a small rank truncation error due to the forcing term. In Figure 3, we can see that the Runge-Kutta BUG integrator achieves second-order convergence. The third- and fourth-order convergences are not visible since the error, around  $10^{-10}$ , is of the order of the machine precision. Moreover, for second-order methods, the error reaches the plateau corresponding to the low-rank truncation, which decreases as the rank increases. Furthermore, the Runge-Kutta BUG integrator is several orders of magnitude more accurate than the projected Runge-Kutta method, which can be explained by the fact that the Galerkin projection is more accurate than the tangent-space projection for approximating the discrete solution.

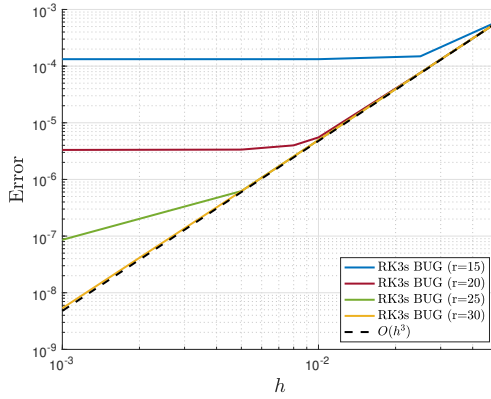




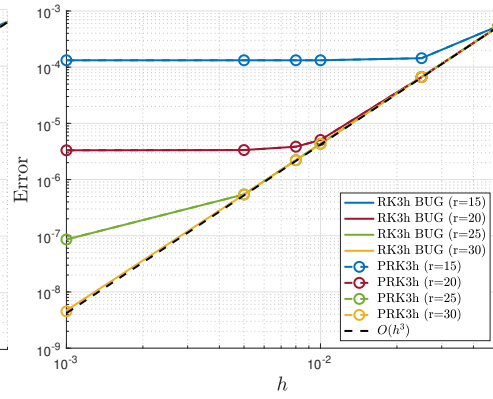
(a) Midpoint method



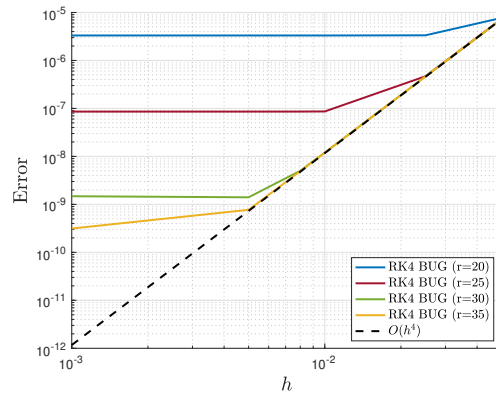
(b) Heun's method



(c) Third-order SSP Runge-Kutta method



(d) Heun's third-order method



(e) Classic fourth-order Runge-Kutta method

**Fig. 1:** Convergence error of the Runge-Kutta BUG integrator for the Allen-Cahn equation

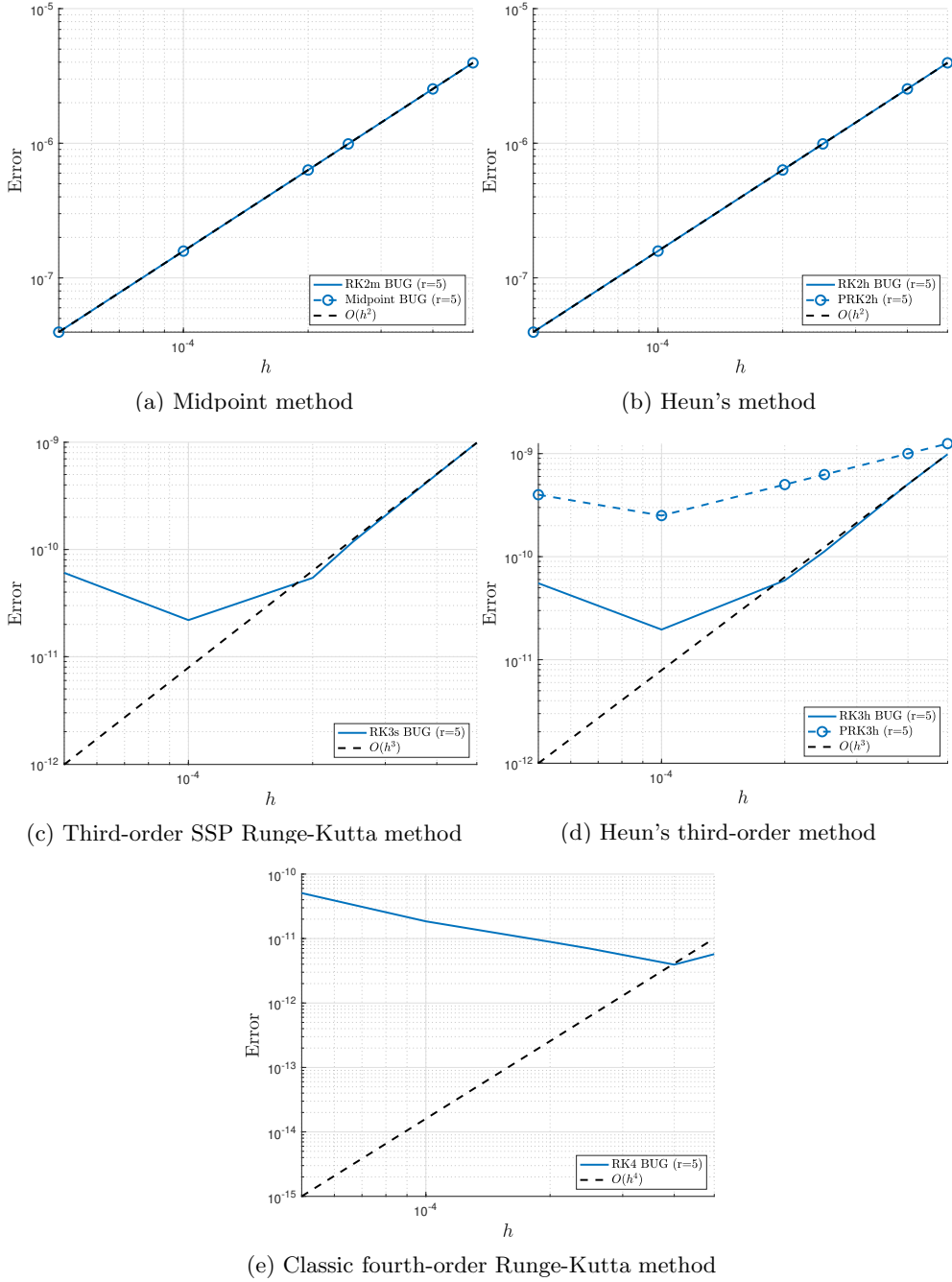
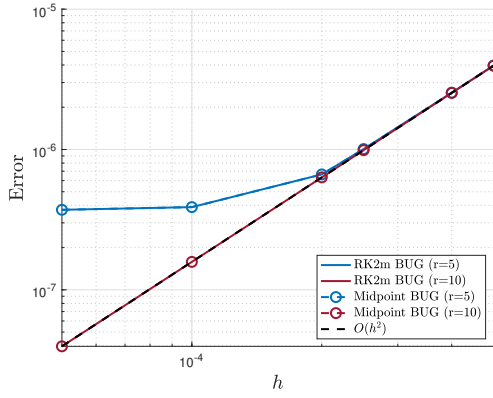
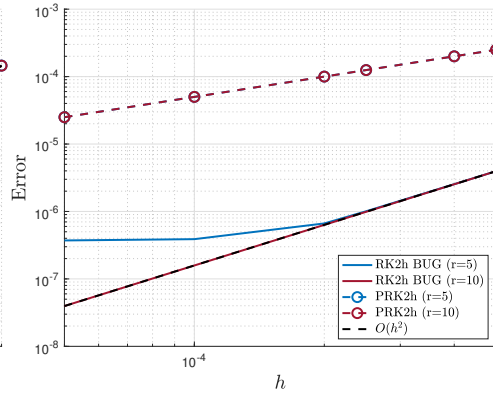


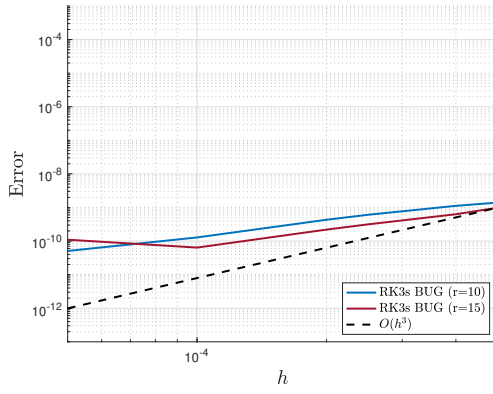
**Fig. 2:** Convergence error of the Runge-Kutta BUG integrator for the Lyapunov equation with  $\theta = 10^{-5}$



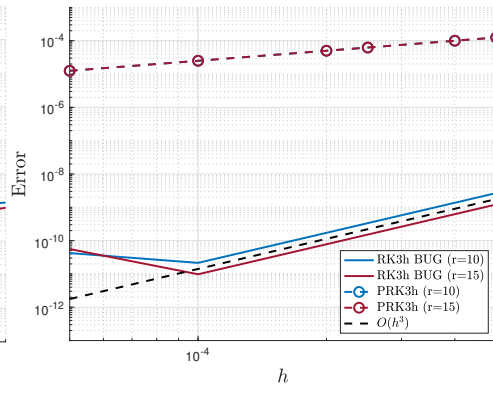
(a) Midpoint method



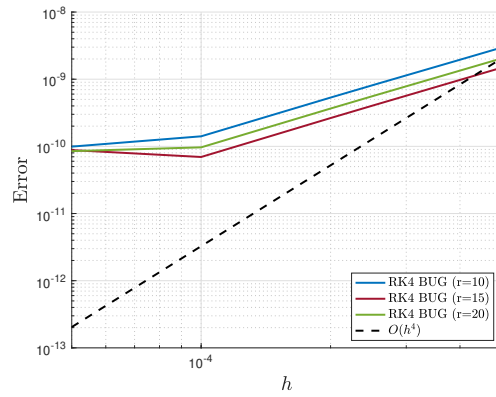
(b) Heun's method



(c) Third-order SSP Runge-Kutta method



(d) Heun's third-order method



(e) Classic fourth-order Runge-Kutta method

**Fig. 3:** Convergence error of the Runge-Kutta BUG integrator for the Lyapunov equation with  $\theta = 1$

### 5.3 Schrödinger equation

Lastly, we consider the Schrödinger equation:

$$\begin{cases} \dot{\mathbf{A}}(t) = 0.5i(\mathbf{D}\mathbf{A}(t) + \mathbf{A}(t)\mathbf{D}) + \theta i|\mathbf{A}(t)|^2 \odot \mathbf{A}(t) \\ \mathbf{A}(0) = \mathbf{A}_0, \end{cases}$$

where  $\mathbf{A}(t) \in \mathbb{R}^{n \times n}$ ,  $\mathbf{D} = \text{diag}(1, 0, 1) \in \mathbb{R}^{n \times n}$ ,  $t \in [0, 5]$ , and  $\theta \geq 0$ . Moreover, we set  $n = 128$ , and the initial solution is given by

$$(\mathbf{A}_0)_{j,l} = \exp\left(-\frac{(j-60)^2}{100} - \frac{(l-50)^2}{100}\right) + \exp\left(-\frac{(j-50)^2}{100} - \frac{(l-40)^2}{100}\right).$$

We start with the case  $\theta = 0.1$ . In Figure 4, we present the error of the Runge-Kutta BUG integrator as a function of the time-step size  $h$  and rank  $r$ . The reader can see that the Runge-Kutta BUG integrator achieves the expected convergence order. Then, the error reaches the plateau resulting from the low-rank truncation and which vanishes as the rank increases. Moreover, the accuracy of the Runge-Kutta BUG integrator is almost the same as that of the midpoint BUG integrator and projected Runge-Kutta method for second-order methods. However, for the Heun's third-order method, the Runge-Kutta BUG integrator is significantly more accurate than the projected Runge-Kutta method.

We now consider the case  $\theta = 0.3$ , where a higher rank is necessary to obtain a small rank truncation error due to the cubic term. In Figure 5, we can see that the error behaves in the same way as before. Note that, for third-order methods, the Runge-Kutta BUG integrator achieves third-order convergence for  $h \leq 10^{-1}$ .

## 6 Conclusion

In this work, we have proposed high-order BUG integrators based on explicit Runge-Kutta methods. By construction, the resulting low-rank integrators are robust to the presence of small singular values and do not involve backward time-integration step. Then, we have analyzed the convergence of the proposed Runge-Kutta BUG integrator. The error bound shows that the Runge-Kutta BUG integrator retains the order of convergence of the associated Runge-Kutta method until the error reaches a plateau resulting from the low-rank truncation and which vanishes as the rank increases.

This error bound has been validated numerically for three different experiments. The results demonstrate the high-order convergence of the Runge-Kutta BUG integrator and its superior accuracy compared to projected Runge-Kutta methods for high orders  $p \geq 3$  and small time-steps.

In perspective, the Runge-Kutta BUG integrator can be extended to other classes of Runge-Kutta methods, such as exponential Runge-Kutta methods or implicit Runge-Kutta methods. These topics will be addressed in future work.

**Acknowledgements.** This work has been supported by the Swiss National Science Foundation under the Project n. 200518 "Dynamical low rank methods for uncertainty quantification and data assimilation".

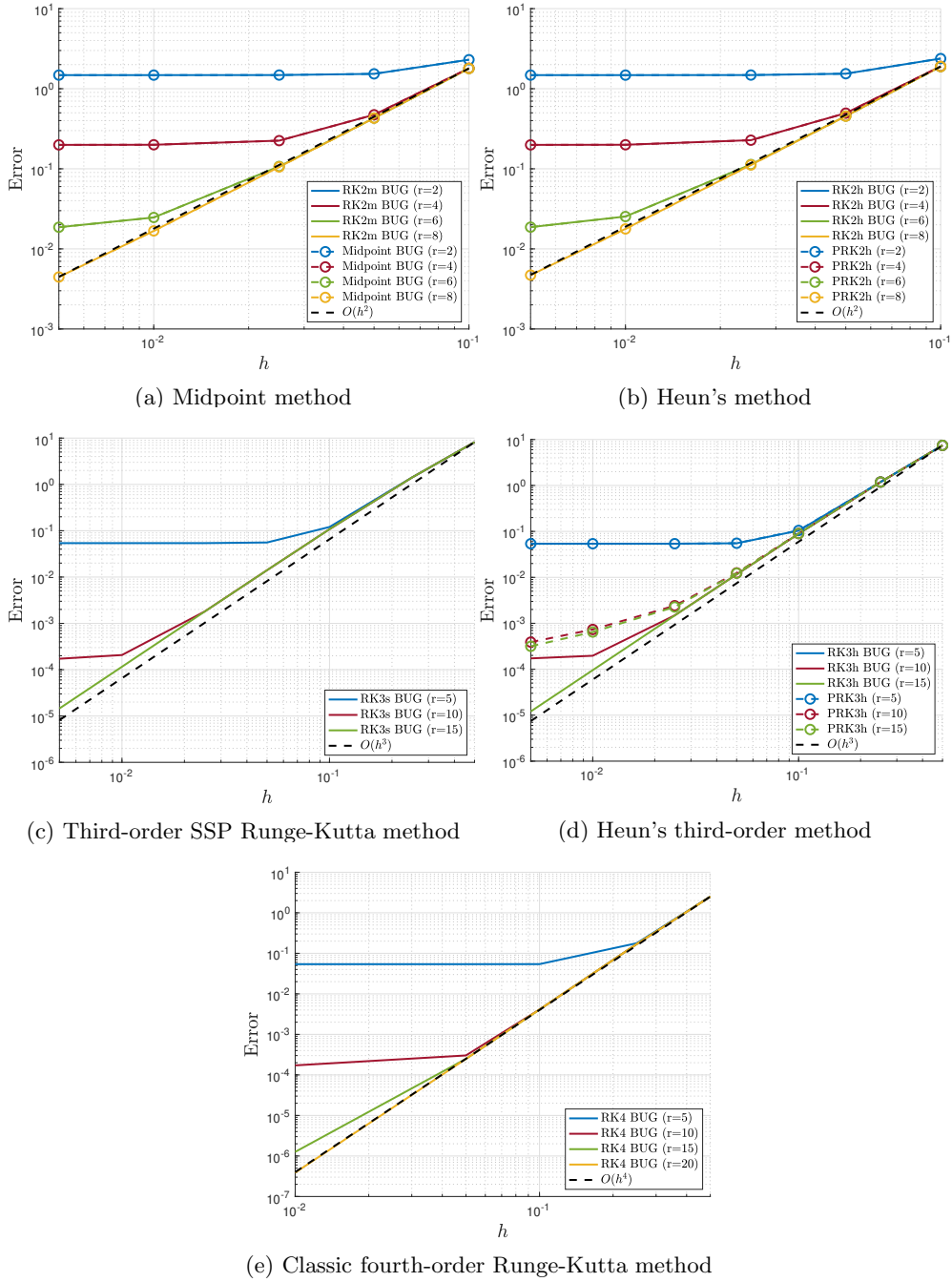


**Fig. 4:** Convergence error of the Runge-Kutta BUG integrator for the Schrödinger equation with  $\theta = 0.1$

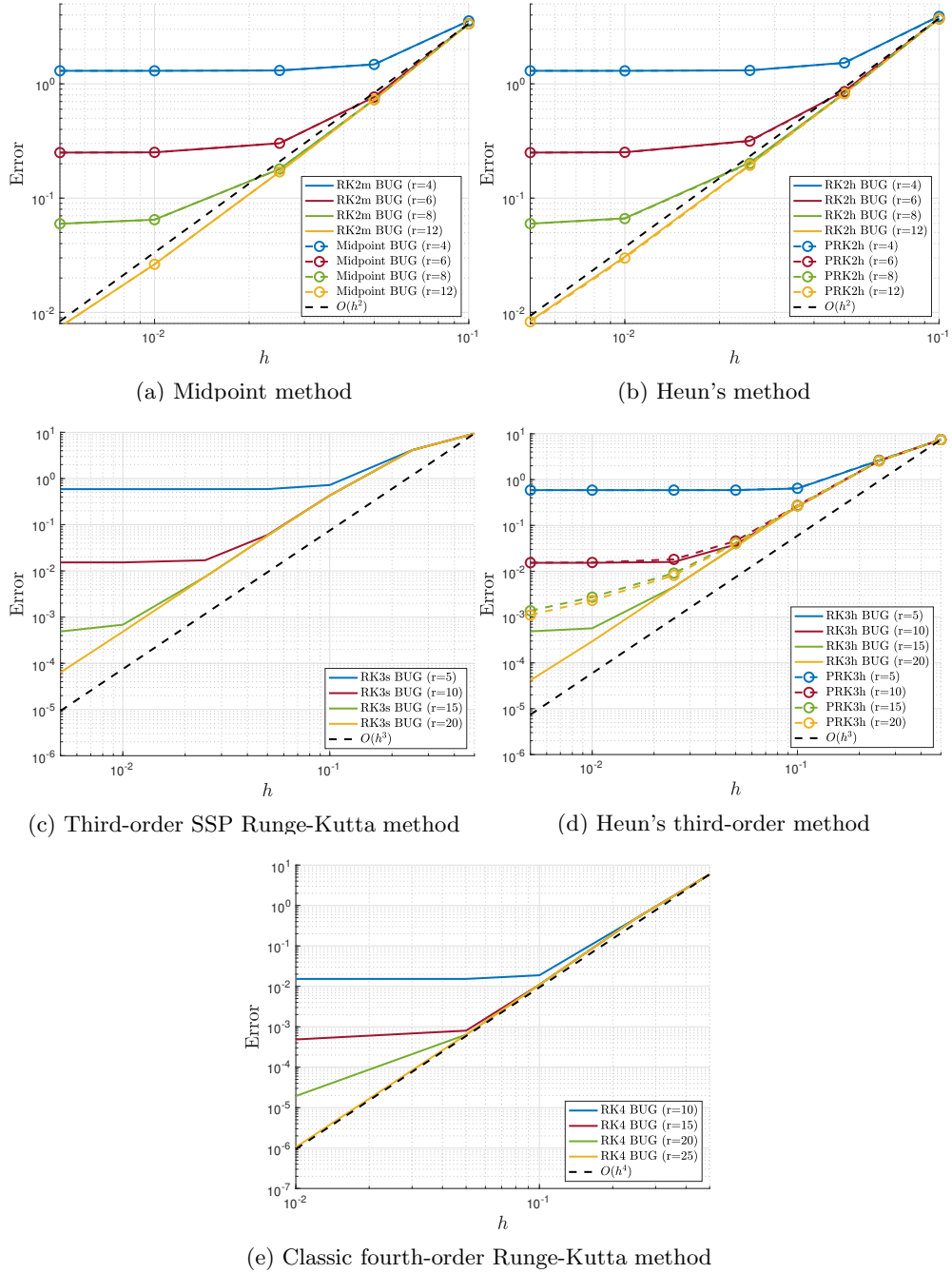


**Fig. 5:** Convergence error of the Runge-Kutta BUG integrator for the Schrödinger equation with  $\theta = 0.3$

## Appendix A List of Runge-Kutta methods

The Butcher tableaux associated with the different Runge-Kutta methods used in this work are listed below.

- Forward Euler method

$$\begin{array}{c|c} 0 & 0 \\ 1 & 1 \\ \hline & 1 \end{array}$$

- Explicit midpoint method

$$\begin{array}{c|cc} 0 & 0 & 0 \\ 1/2 & 1/2 & 0 \\ \hline & 0 & 1 \end{array}$$

- Heun's method

$$\begin{array}{c|cc} 0 & 0 & 0 \\ 1 & 1 & 0 \\ \hline & 1/2 & 1/2 \end{array}$$

- Third-order SSP Runge-Kutta method

$$\begin{array}{c|ccc} 0 & 0 & 0 & 0 \\ 1 & 1 & 0 & 0 \\ 1/2 & 1/4 & 1/4 & 0 \\ \hline & 1/6 & 1/6 & 2/3 \end{array}$$

- Heun's third-order method

$$\begin{array}{c|ccc} 0 & 0 & 0 & 0 \\ 1/3 & 1/3 & 0 & 0 \\ 2/3 & 0 & 2/3 & 0 \\ \hline & 1/4 & 0 & 3/4 \end{array}$$

- Classic fourth-order Runge-Kutta method

$$\begin{array}{c|cccc} 0 & 0 & 0 & 0 & 0 \\ 1/2 & 1/2 & 0 & 0 & 0 \\ 1/2 & 0 & 1/2 & 0 & 0 \\ 1 & 0 & 0 & 1 & 0 \\ \hline & 1/6 & 1/3 & 1/3 & 1/6 \end{array}$$

## References

- [1] Ceruti, G., Kusch, J., Lubich, C.: A rank-adaptive robust integrator for dynamical low-rank approximation. *BIT Numerical Mathematics* **62**(4), 1149–1174 (2022)
- [2] Bernard, F., Iollo, A., Riffaud, S.: Reduced-order model for the BGK equation based on POD and optimal transport. *Journal of Computational Physics* **373**, 545–570 (2018)

- [3] Einkemmer, L., Lubich, C.: A low-rank projector-splitting integrator for the Vlasov–Poisson equation. *SIAM Journal on Scientific Computing* **40**(5), 1330–1360 (2018)
- [4] Einkemmer, L., Ostermann, A., Piazzola, C.: A low-rank projector-splitting integrator for the Vlasov–Maxwell equations with divergence correction. *Journal of Computational Physics* **403**, 109063 (2020)
- [5] Einkemmer, L., Joseph, I.: A mass, momentum, and energy conservative dynamical low-rank scheme for the Vlasov equation. *Journal of Computational Physics* **443**, 110495 (2021)
- [6] Coughlin, J., Hu, J.: Efficient dynamical low-rank approximation for the Vlasov–Ampere–Fokker–Planck system. *Journal of Computational Physics* **470**, 111590 (2022)
- [7] Einkemmer, L.: Accelerating the simulation of kinetic shear Alfvén waves with a dynamical low-rank approximation. *Journal of Computational Physics* **501**, 112757 (2024)
- [8] Einkemmer, L., Kormann, K., Kusch, J., McClarren, R.G., Qiu, J.-M.: A review of low-rank methods for time-dependent kinetic simulations
- [9] Sapsis, T.P., Lermusiaux, P.F.: Dynamically orthogonal field equations for continuous stochastic dynamical systems. *Physica D: Nonlinear Phenomena* **238**(23–24), 2347–2360 (2009)
- [10] Babae, H., Choi, M., Sapsis, T.P., Karniadakis, G.E.: A robust bi-orthogonal/dynamically-orthogonal method using the covariance pseudo-inverse with application to stochastic flow problems. *Journal of Computational Physics* **344**, 303–319 (2017)
- [11] Musharbash, E., Nobile, F.: Dual dynamically orthogonal approximation of incompressible Navier Stokes equations with random boundary conditions. *Journal of Computational Physics* **354**, 135–162 (2018)
- [12] Feppon, F., Lermusiaux, P.F.: Dynamically orthogonal numerical schemes for efficient stochastic advection and Lagrangian transport. *Siam Review* **60**(3), 595–625 (2018)
- [13] Musharbash, E., Nobile, F., Vidličková, E.: Symplectic dynamical low rank approximation of wave equations with random parameters. *BIT Numerical Mathematics* **60**(4), 1153–1201 (2020)
- [14] Patil, P., Babae, H.: Real-time reduced-order modeling of stochastic partial differential equations via time-dependent subspaces. *Journal of Computational Physics* **415**, 109511 (2020)



- [15] Kazashi, Y., Nobile, F.: Existence of dynamical low rank approximations for random semi-linear evolutionary equations on the maximal interval. *Stochastics and Partial Differential Equations: Analysis and Computations* **9**(3), 603–629 (2021)
- [16] Kazashi, Y., Nobile, F., Vidličková, E.: Stability properties of a projector-splitting scheme for dynamical low rank approximation of random parabolic equations. *Numerische Mathematik* **149**, 973–1024 (2021)
- [17] Kazashi, Y., Nobile, F., Zoccolan, F.: Dynamical low-rank approximation for stochastic differential equations. *Mathematics of Computation* (2024)
- [18] Kressner, D., Tobler, C.: Low-rank tensor Krylov subspace methods for parametrized linear systems. *SIAM Journal on Matrix Analysis and Applications* **32**(4), 1288–1316 (2011)
- [19] Weinhandl, R., Benner, P., Richter, T.: Linear Low-Rank Parameter-Dependent Fluid-Structure Interaction Discretization in 2D. *PAMM* **18**(1), 201800178 (2018)
- [20] Benner, P., Richter, T., Weinhandl, R.: A low-rank method for parameter-dependent fluid-structure interaction discretizations with hyperelasticity. *ZAMM-Journal of Applied Mathematics and Mechanics/Zeitschrift für Angewandte Mathematik und Mechanik* **104**(10), 202300562 (2024)
- [21] Riffaud, S., Fernández, M.A., Lombardi, D.: A Low-Rank Solver for Parameter Estimation and Uncertainty Quantification in Time-Dependent Systems of Partial Differential Equations. *Journal of Scientific Computing* **99**(2), 34 (2024)
- [22] Koch, O., Lubich, C.: Dynamical low-rank approximation. *SIAM Journal on Matrix Analysis and Applications* **29**(2), 434–454 (2007)
- [23] Lubich, C., Oseledets, I.V.: A projector-splitting integrator for dynamical low-rank approximation. *BIT Numerical Mathematics* **54**(1), 171–188 (2014)
- [24] Kieri, E., Lubich, C., Walach, H.: Discretized dynamical low-rank approximation in the presence of small singular values. *SIAM Journal on Numerical Analysis* **54**(2), 1020–1038 (2016)
- [25] Kusch, J., Einkemmer, L., Ceruti, G.: On the stability of robust dynamical low-rank approximations for hyperbolic problems. *SIAM Journal on Scientific Computing* **45**(1), 1–24 (2023)
- [26] Ceruti, G., Lubich, C.: An unconventional robust integrator for dynamical low-rank approximation. *BIT Numerical Mathematics* **62**(1), 23–44 (2022)
- [27] Ceruti, G., Kusch, J., Lubich, C.: A parallel rank-adaptive integrator for dynamical low-rank approximation. *SIAM Journal on Scientific Computing* **46**(3), 205–228 (2024)

- [28] Kieri, E., Vandereycken, B.: Projection methods for dynamical low-rank approximation of high-dimensional problems. *Computational Methods in Applied Mathematics* **19**(1), 73–92 (2019)
- [29] Carrel, B., Vandereycken, B.: Projected exponential methods for stiff dynamical low-rank approximation problems. arXiv preprint arXiv:2312.00172 (2023)
- [30] Ceruti, G., Einkemmer, L., Kusch, J., Lubich, C.: A robust second-order low-rank BUG integrator based on the midpoint rule. *BIT Numerical Mathematics* **64**(3), 30 (2024)
- [31] Kusch, J.: Second-order robust parallel integrators for dynamical low-rank approximation. arXiv preprint arXiv:2403.02834 (2024)
- [32] Einkemmer, L., Kusch, J., Schotthöfer, S.: Conservation properties of the augmented basis update & Galerkin integrator for kinetic problems. arXiv preprint arXiv:2311.06399 (2023)
- [33] Harrier, E., Norsett, S., Wanner, G.: *Solving Ordinary Differential Equations I: Nonstiff Problems*, (1993)
- [34] Eckart, C., Young, G.: The approximation of one matrix by another of lower rank. *Psychometrika* **1**(3), 211–218 (1936)
- [35] Horn, R.A., Johnson, C.R.: *Topics in Matrix Analysis*, (1991)
- [36] Lam, H.Y., Ceruti, G., Kressner, D.: Randomized low-rank runge-kutta methods. arXiv preprint arXiv:2409.06384 (2024)

